3-1-1988

Stability of Steady Cross-waves: Theory and Experiment

Seth Lichter
University of Arizona

Andrew J. Bernoff
Harvey Mudd College

Stability of steady cross waves: Theory and experiment

Seth Lichter
Department of Aerospace and Mechanical Engineering, University of Arizona, Tucson, Arizona 85721

Andrew J. Bernoff
Department of Mathematics, University of Arizona, Tucson, Arizona 85721

(Received 17 August 1987)

A bifurcation analysis is performed in the neighborhood of neutral stability for cross waves as a function of forcing, detuning, and viscous damping. A transition is seen from a subcritical to a supercritical bifurcation at a critical value of the detuning. The predicted hysteretic behavior is observed experimentally. A similarity scaling in the inviscid limit is also predicted. The experimentally observed bifurcation curves agree with this scaling.

I. INTRODUCTION

Jones[1] derived the nonlinear Schrödinger equation (NLS) which governs the evolution of parametrically excited inviscid cross waves (see also Miles[2]). The coefficients in the NLS are modified by viscous effects due to the boundary layers on the sidewalls, bottom, and free surface.[3] These works only consider the linear stability of cross waves. Miles and Becker[4] recently derived an approximate nonlinear solution to the viscous cross-wave equations; their work suggests the existence of multiple steady solutions and suggests the possibility of hysteretic behavior.

Barnard and Pritchard[5] were unable to observe steady cross waves experimentally. Lichter and Shemer[6] observed steady cross waves at small forcing and modulated waves at large forcing. The unsteadiness at large forcing was associated with a soliton which propagated away from the wave maker. Shemer and Lichter[7] identified steady, quasiperiodic, and chaotic cross waves as a function of detuning and forcing amplitude. Lichter and Underhill[8] observed chaotic cross waves under conditions in which two spatial modes appeared to be unstable.

In this paper, a bifurcation analysis is performed in the neighborhood of neutral stability. A transition from a supercritical to a subcritical pitchfork bifurcation is found, indicating the presence of hysteresis. In the inviscid region, a similarity scaling is identified. Experimental results confirming these predictions are presented. The experiments yield a number of observations (e.g., a bifurcation to quasiperiodic behavior) which, as yet, are unresolved.

The equations of motion are presented in Sec. II. A bifurcation analysis is performed in Sec. III. The inviscid similarity scaling is discussed in Sec. IV. The experimental facility is described in Sec. V. A discussion of the results and their comparison with experiment are contained in Sec. VI. These results are summarized in Sec. VII.

II. FORMULATION

The inviscid modulation equations governing the onset of cross waves in a long channel were first derived by Jones.[1] Lichter and Chen[9] found it necessary to account for viscous effects in order to achieve quantitative agreement of theory and experiment; they augmented Jones's equation with a linear damping term. Bernoff *et al.*[3] formally derived the viscous modifications due to the sidewalls, bottom, and free-surface boundary layers.

It is convenient to write the governing NLS for complex cross-wave amplitude, A, as two real equations, using $A=C+iD$ (cf. Jones[1]). Suitably transformed, the equations and boundary conditions may be written as

$$\underline{C}_T=\mathcal{L}\underline{C}+\mathcal{N}(\underline{C})\ , \tag{2.1a}$$

$$\underline{C}_X=\mathcal{B}\underline{C} \quad \text{at } X=0\ . \tag{2.1b}$$

Here, the vector $\underline{C}$ is defined by

$$\underline{C}=\begin{bmatrix} C \\ D \end{bmatrix}\ , \tag{2.2}$$

and the operators $\mathcal{L}$, $\mathcal{N}$, and $\mathcal{B}$ are

$$\mathcal{L}=\begin{bmatrix} -L & -\lambda-\partial_{XX} \\ \lambda+\partial_{XX} & -L \end{bmatrix}\ , \tag{2.3a}$$

$$\mathcal{N}(\underline{C})=\begin{bmatrix} -(C^2+D^2)D \\ (C^2+D^2)C \end{bmatrix}\ , \tag{2.3b}$$

and

$$\mathcal{B}=\begin{bmatrix} 1 & 0 \\ 0 & -1 \end{bmatrix}\ . \tag{2.3c}$$

The slow spatial and temporal variables are X and T, respectively. The detuning, λ, is defined by

$$\lambda=\frac{4}{(\epsilon R)^2}\left[\frac{f}{f_0}-1\right]\ , \tag{2.4}$$

where the contributions from the progressiving wave[1] and viscosity[3] are ignored as they are small. The nondimensional forcing, ε, is given by the wave-maker forcing amplitude a scaled by the cross-wave wavelength $W/N\pi$,

$$\varepsilon=\frac{a}{W/N\pi} , \tag{2.5}$$

where W is the tank width and N is the mode number. The numerical factor R accounts for wave-maker shape.[9] The forcing frequency f is given in hertz, and the cutoff frequency is given by

$$f_0=\frac{1}{2\pi}\left[\frac{gN\pi}{W}+\frac{T}{\rho}\left[\frac{N\pi}{W}\right]^3\right]^{1/2} , \tag{2.6}$$

where T is surface tension and ρ is density. Surface tension effects are presumed to have a negligible effect on Eq. (2.1) but have a measurable effect on the cutoff frequency at the forcing frequencies used. The effective damping L,

$$L=\frac{2}{(\varepsilon R)^2\mathcal{R}}\left[4+\frac{2\sqrt{2\mathcal{R}}}{N\pi}\right] , \tag{2.7}$$

measures the viscous dissipation scaled by the energy input at the wave maker.[3] The contributions to L from the bottom- and boundary-layer interaction have been omitted as they are small. The Reynolds number is

$$\mathcal{R}\simeq\frac{2f_0W^2}{\nu N^2\pi^2} , \tag{2.8}$$

where ν is the kinematic viscosity.

III. BIFURCATION ANALYSIS

In this section, a bifurcation analysis is performed in the neighborhood of the neutral stability curve. The stability of the zero state is governed by the linear stability problem,

$$\sigma\underline{C}=\mathcal{L}\underline{C} , \tag{3.1a}$$

$$\underline{C}_X=\mathcal{B}\underline{C} \quad \text{at } X=0 , \tag{3.1b}$$

where σ is the eigenvalue.

This eigenvalue problem can be used to define a projection formalism that will allow the evolution in the direction of particular eigenvectors to be examined.[3,10,11] First, define an inner product,

$$\langle\underline{C}'\cdot\underline{C}\rangle=\int_0^\infty (C'C+D'D)dX . \tag{3.2}$$

The adjoint problem is defined as

$$\mathcal{L}^\dagger\underline{C}=\sigma\underline{C} , \tag{3.3a}$$

$$\underline{C}_X=\mathcal{B}^\dagger\underline{C} , \tag{3.3b}$$

which must satisfy the identity

$$\langle\underline{C}',\mathcal{L}\underline{C}\rangle=\langle\mathcal{L}^\dagger\underline{C}',\underline{C}\rangle . \tag{3.4}$$

Integration by parts yields

$$\mathcal{L}^\dagger=\mathcal{P}^{-1}\mathcal{L}\mathcal{P} , \tag{3.5}$$

$$\mathcal{B}^\dagger=\mathcal{P}^{-1}\mathcal{B}\mathcal{P} , \tag{3.6}$$

where $\mathcal{P}$ is the matrix which transposes C and D,

$$\mathcal{P}=\begin{bmatrix}0&1\\1&0\end{bmatrix} . \tag{3.7}$$

The eigenvectors of Eq. (3.1) can be found as a finite linear combination of complex exponentials. Here, only the most unstable eigenvector, $\underline{C}_0$, needs to be considered. Following Jones[1] and Bernoff *et al.*,[3] $\underline{C}_0$ takes the form

$$\underline{C}_0=\kappa\begin{bmatrix} i(\alpha^*-1)e^{\alpha X}+\text{c.c.}\\ -(\alpha^*-1)e^{\alpha X}+\text{c.c.}\end{bmatrix} , \tag{3.8}$$

$$\kappa^{-2}=8\left[1+\left[\frac{1-\lambda}{2}\right]^{1/2}\right] , \tag{3.9}$$

where κ has been chosen to normalize $|\underline{C}_0|=1$ at $X=0$, and

$$\alpha=-\frac{1}{\sqrt{2}}(\sqrt{1-\lambda}+i\sqrt{1+\lambda}) . \tag{3.10}$$

The associated eigenvalue is given by

$$\sigma_0=-L+(1-\lambda^2)^{1/2} . \tag{3.11}$$

The bifurcation analysis is considered in the neighborhood of the neutral stability curve ($\sigma_0=0$). Here, $|\sigma_0|\ll 1$ and, consequently, a perturbation in the $\underline{C}_0$ direction will evolve slowly. The remaining eigenvalues of $\mathcal{L}$ have negative real parts of order L and, as such, correspond to relatively rapidly damped modes. Given an initial condition of small amplitude, the portion of the solution corresponding to the damped eigenvectors will decay quickly. The solution will become attracted to a one-dimensional center manifold[12] tangent to $\underline{C}_0$ at $\underline{C}=0$. Therefore, the amplitude $\underline{C}$ can be approximated at leading order by

$$\underline{C}=r(t)\underline{C}_0 , \tag{3.12}$$

where $r(t)$ is a time-dependent amplitude. The equation of motion for $r(t)$ can now be found by substituting Eq. (3.12) into Eq. (2.1) and projecting onto the direction of $\underline{C}_0$. This can be done by defining the adjoint eigenvector $\underline{C}_0^\dagger$,

$$\mathcal{L}^\dagger\underline{C}_0^\dagger=\sigma_0\underline{C}_0^\dagger , \tag{3.13}$$

and then using the operator $\langle\underline{C}_0^\dagger,\cdot\rangle$ to project onto the $\underline{C}_0$ subspace. This yields the Landau equation,

$$r_t-\sigma_0 r=Hr^3 , \tag{3.14}$$

where the Landau constant H is defined by

$$H=\frac{\langle\underline{C}_0^\dagger,\mathcal{N}(\underline{C}_0)\rangle}{\langle\underline{C}_0^\dagger,\underline{C}_0\rangle} , \tag{3.15}$$

and $\mathcal{N}$ is defined in Eq. (2.3b). Equations (3.5) and (3.6) yield the identity

$$\underline{C}_0^\dagger=\mathcal{P}\underline{C}_0 , \tag{3.16}$$

which allows the evaluation of Eq. (3.15),

$$H=\frac{1-3\lambda}{5-3\lambda}\frac{1}{(1-\lambda^2)^{1/2}} . \tag{3.17}$$

Note that as $\mathcal{N}$ is cubic at leading order, the damped eigenvectors will not contribute to the Landau equation until order r^5 (Ref. 13).

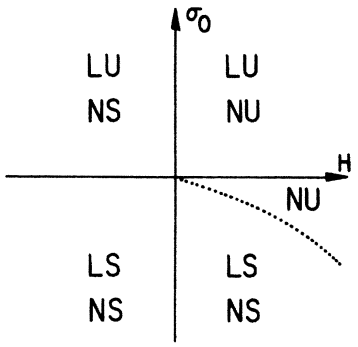

FIG. 1. Behavior of the Landau equation as a function of the eigenvalue σ_0 and the Landau constant H. The regimes of linear stability (LS), nonlinear stability (NS), linear instability (LU), and nonlinear instability (NU) are shown. The dotted curve indicates the locus of the saddle-node bifurcation in the case when the fifth-order correction is stabilizing.

The dynamics of the Landau equation [Eq. (3.14)] may be studied as a function of the independent parameters σ_0 and H (Fig. 1). For $H<0$ (i.e., $\lambda>\frac{1}{3}$), the bifurcation is a supercritical pitchfork [Fig. 2(a)]. For $\sigma_0<0$, the solution is both linearly and nonlinearly stable. For $\sigma_0>0$, the solution is linearly unstable, and the nonlinear term is stabilizing and leads to saturation. The saturation amplitude, r_s, of the cross wave can be computed by setting $r_t=0$ in Eq. (3.14) and solving to yield

$$r_s=\left[-\frac{\sigma_0}{H}\right]^{1/2}. \tag{3.18}$$

When $H>0$ (i.e., $\lambda<\frac{1}{3}$), the bifurcation is a subcritical pitchfork [Fig. 2(b)]. When $\sigma_0>0$, the nonlinear term augments the linear growth term and the solution grows without bound. When $\sigma_0<0$, the behavior is hysteretic:

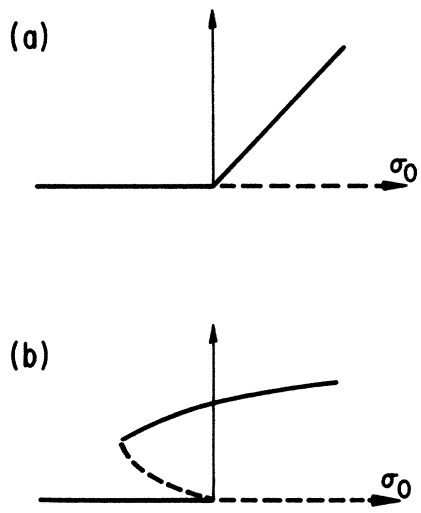

FIG. 2. Wave height squared of the most unstable eigenvectors as a function of the eigenvalue σ_0 for (a) supercritical ($H<0$) and (b) subcritical solutions ($H>0$). Solid lines show stable solutions, and dashed lines are unstable solutions.

for the $|r|<r_s$, the solution will decay to zero; for $|r|>r_s$, the solution will grow due to the influence of the nonlinear terms.

For $|H|\ll 1$, the fifth-order correction to Eq. (3.14) will become important. In the case when this term is stabilizing, the subcritical branch terminates in a saddle-node bifurcation [Fig. 2(b)]. The locus of the saddle-node bifurcation is given by $\sigma_0=-\gamma H^2$ for some constant $\gamma>0$ (Ref. 12) (cf. Fig. 1).

IV. INVISCID THEORY

In the limit $L\ll\lambda$, the dynamics of cross waves are dominated by the inviscid effects.[3] For fixed Reynolds number, this corresponds to the limit of large forcing, ε. If this limit is regular, bifurcations should only depend upon λ at leading order. Assuming that a bifurcation occurs at some λ_c, then it follows from Eq. (2.4) that, considered as a function of ε and f, the bifurcation will occur on the curve

$$\varepsilon^2=\frac{4}{\lambda_c R^2}\left[\frac{f}{f_0}-1\right].$$

This suggests that $(f/f_0-1,\varepsilon^2)$ may be convenient experimental parameters; with these coordinates, bifurcation curves should asymptote to straight lines in the limit of large ε.

In this limit, comparison can also be made to the work of Miles and Becker.[4] They derived an exact solution to the steady cross-wave profile in terms of a trapped soliton when $-\lambda>1$ (corresponding to $\sigma_0<0$, $H>0$). When $\lambda\to-1$ ($\sigma_0\to 0$), the solution reproduces the subcritical branch described above [Eq. (3.18)] and, as such, this branch is unstable near the bifurcation point.

V. EXPERIMENTAL FACILITY

Experiments were carried out in a wave tank 120 cm long and $W=30.97$. The wave maker is a paddle-type, where the hinge of the paddle is at a depth of 14.1 cm on a pedestal which is raised 13.1 cm from the bottom. The wave maker is driven by a moving coil linear actuator. The input sine wave is computer generated with 100 points per period, passed through a digital-to-analog converter and then amplified. Frequency stability was better than one part in 10^5. Wave-maker displacement is measured by a noncontact inductance transducer. This transducer also serves as input into a feedback loop providing proportional and derivative feedback to ensure that the input sinusoidal waveform is faithfully reproduced. Wave height is measured by a capacitance-type wave probe. The probe wire is only 0.8 mm in diameter, so wave interference is negligible even for the shortest progressing waves generated at a forcing frequency of 8.16 Hz (3.0 cm wavelength). The probe was positioned one-half cross-wave wavelength away from one sidewall (and so at the location of a cross-wave crest) and 1.7 cm distant from the mean position of the wave maker. Experiments were carried out over a range of frequencies, 7.6–8.16 Hz, for which the dominant spatial mode number is $N=6$.

To reduce capillary effects at the walls and on the wave maker, Kodak Corporation's Photo-Flo was added to the water. Sufficient Photo-Flo was added so that additional solution had a negligible effect on surface tension. This limiting value of 33.3-dyn/cm surface tension was measured by the DuHouy ring technique.

VI. DISCUSSION AND COMPARISON WITH EXPERIMENT

In contrast to the analytical theory where σ_0 and H arise naturally, it is most feasible to conduct an experiment at constant forcing amplitude or constant forcing frequency. The results in Fig. 3 are considered as functions of ε and f; all other experimental parameters were held constant. It is convenient to choose $(f/f_0-1,\varepsilon^2)$ as coordinates (cf. Sec. IV). Curves of constant λ appear as lines radiating from the origin. The neutral stability curve, on which $\sigma_0=0$, can be rewritten using Eqs. (2.4) and (2.7) as

$$(\varepsilon R)^4-16\left[\frac{f}{f_0}-1\right]^2=\left[\frac{2}{\mathcal{R}}\left[4+\frac{2\sqrt{2\mathcal{R}}}{N\pi}\right]\right]^2.$$

With these coordinates, this curve is a hyperbola with asymptotes on which $\lambda=\pm1$. The slope of the asymptotes yields the experimental value of R. In Fig. 3(a), the solid line is the theoretical prediction of $\lambda=\frac{1}{3}$; to the left of this line, hysteresis is expected in the neighborhood of the neutral stability curve.

The solid upward-pointing triangles in Fig. 3(a) indicate the appearance of cross waves for increasing wavemaker amplitude, whereas the downward-pointing triangles mark the disappearance of cross waves with decreas-

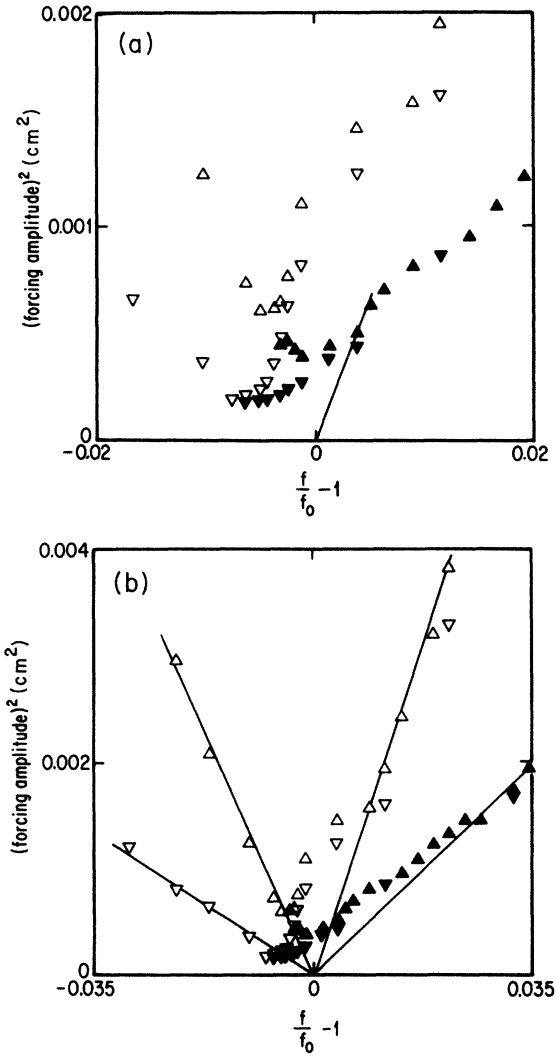

FIG. 3. Stability diagram for the experimental results. The open symbols denote that the cross waves were modulated on a long time scale. The solid symbols denote unmodulated waves. The up-pointing (down-pointing) triangles indicate that the forcing amplitude was increased (decreased) at constant forcing frequency. (a) Close-up of the hysteresis region and the theoretical prediction $\lambda=\frac{1}{3}$ (— — —). (b) The straight lines converging to the inviscid cutoff frequency reveal the similarity scaling of the inviscid limit.

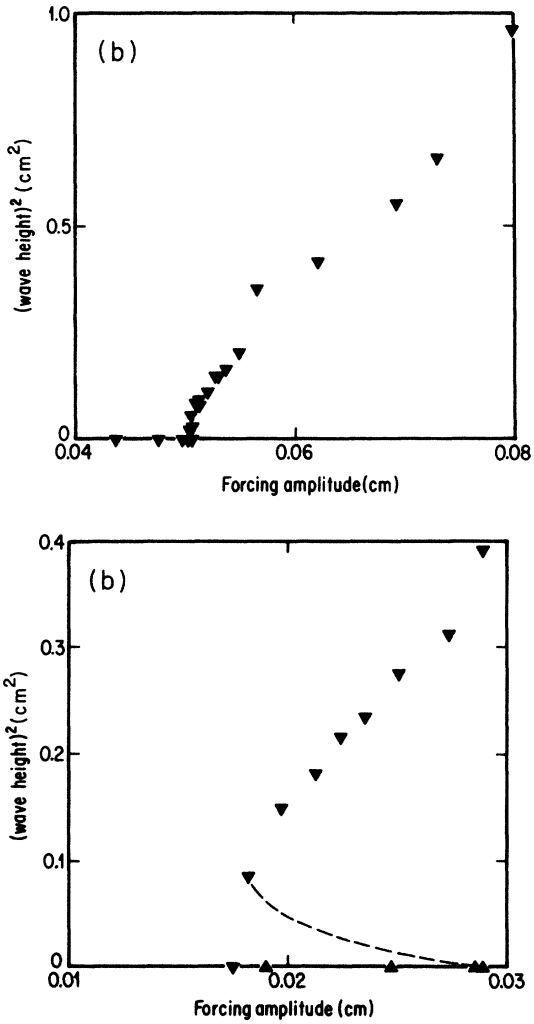

FIG. 4. Wave height squared as a function of forcing amplitude for (a) 8.1 Hz showing behavior similar to the supercritical case, Fig. 2(a), and (b) for 7.81 Hz showing behavior similar to the subcritical solution, Fig. 2(b). The dashed line is hypothesized.

ing wave-maker amplitude. To the left of the line $\lambda=\frac{1}{3}$, these two curves diverge, indicating the appearance of hysteretic behavior in agreement with the prediction of Sec. III. Figure 4 shows cross-wave amplitude as a function of wave-maker forcing at constant detuning. In Fig. 4(a), a detuning to the right of the hysteretic transition is shown; note that a bifurcation to a steady cross wave is observed, in agreement with Fig. 2(a). In Fig. 4(b), a detuning to the left of the hysteretic transition is shown; here, a stable zero solution and a stable steady cross wave exist at the same parameter values, in agreement with Fig. 2(b).

Although the results discussed in Fig. 4 qualitatively reproduce the behavior predicted in Sec. III, a quantitative agreement between the prediction and observed cross-wave amplitude cannot be produced. This indicates that the Landau analysis may be quantitatively valid only in a narrow band along the neutral stability curve. It is speculated that, in the inviscid regime, a slowly decaying cnoidal solution to the full NLS may provide better agreement.

In Fig. 3, the open triangles denote a transition to quasiperiodicity. The upward-pointing triangles to the left of $\lambda=0$ indicate a transition from the zero state to a quasiperiodic cross wave, i.e., modulated on a slow time scale. This transition is hysteretic; if the forcing amplitude is decreased after the quasiperiodic cross waves appear, the waves persist. The downward-pointing open triangles indicate the forcing amplitude below which the quasiperiodic cross waves decay.

A second boundary indicating the transition from steady to quasiperiodic cross waves is also shown by open triangles. A smaller hysteretic effect is also observed on this boundary. Similar behavior was observed by Shemer and Lichter.[7]

For $\lambda \gg L$, the analysis in Sec. IV indicates that inviscid effects should dominate and the various bifurcation curves may be approximated by straight lines. Figure 3(b) shows that all the transition curves qualitatively agree with this scaling.

VII. CONCLUSIONS

An analysis has been presented revealing a bifurcation from supercritical to subcritical behavior for viscous cross waves as a function of forcing amplitude and detuning. The bifurcation occurs at a detuning of $\lambda=\frac{1}{3}$. In the subcritical region, there is a range for which the cross waves are linearly stable but nonlinearly unstable, yielding a hysteretic stability boundary. In the region where $\lambda \gg L$, λ is the single parameter relevant to cross-wave growth, and bifurcations appear as lines when graphed as functions of $(f/f_0-1,\epsilon^2)$. The theoretical predictions are in qualitative agreement with experiment. The experiments also suggest, however, that the range of validity of the Landau analysis is restricted to the proximity of the neutral stability curve.

ACKNOWLEDGMENTS

This work was sponsored by the National Science Foundation and by the U.S. Office of Naval Research.

[1]A. F. Jones, J. Fluid Mech. **138**, 53 (1984).
[2]J. W. Miles, J. Fluid Mech. **151**, 391 (1985).
[3]A. J. Bernoff, L. P. Kwok, and S. Lichter (unpublished).
[4]J. Miles and J. Becker (unpublished).
[5]B. J. S. Barnard and W. G. Pritchard, J. Fluid Mech. **55** (Pt. 2), 245 (1972).
[6]S. Lichter and L. Shemer, Phys. Fluids **29**, 3971 (1986).
[7]L. Shemer and S. Lichter Phys. Fluids **30**, 3427 (1987).
[8]S. Lichter and W. B. Underhill, Phys. Rev. A **35**, 5282 (1987).
[9]S. Lichter and J. Chen, J. Fluid Mech. **183**, 451 (1987).
[10]H. Haken, *Synergetics*, 2nd ed. (Springer-Verlag, New York, 1978).
[11]P. Coullet and E. A. Spiegel, SIAM J. Appl. Math. **43**, 776 (1983).
[12]S. Guckenheimer and P. Holmes, *Nonlinear Oscillations, Dynamical Systems and Bifurcations of Vector Fields* (Springer-Verlag, New York, 1983).
[13]A. J. Bernoff, Ph.D. thesis, University of Cambridge, 1986.